EurJOC European Journal of Organic Chemistry

FULL PAPER

DOI: 10.1002/ejoc.201402068

Mono- vs. Dinuclear Gold-Catalyzed Intermolecular Hydroamidation

Juan M. Serrano-Becerra,[a][‡] Alexander F. G. Maier,[a][‡] Sandra González-Gallardo,[b] Eric Moos,[b] Christoph Kaub,[b] Maximilian Gaffga,[c] Gereon Niedner-Schatteburg,[c] Peter W. Roesky,[b] Frank Breher,[b] and Jan Paradies*[a]

Keywords: Homogeneous catalysis / Gold / Hydroamination / Dinuclear complexes / Cooperative effects

Mono- and dinuclear gold catalysts were investigated in the intermolecular hydroamidation of olefins. Upon activation of [Ph_3PAuCl] and [xantphos($AuCl)_2$] with various silver salts (AgOTf, Ag[BF_4], and Ag[SbF_6]), diverging reactivity of the resulting cationic gold complexes was observed. It was found that both the binding ability of the counterion and the solvent have a significant impact on the reactivity of the mono- and dinuclear complexes.

Introduction

Multimetallic complexes have shown increased reactivity combined with excellent dia- and stereoselectivity when used as homogeneous catalysts in organic transformations.[1] Impressive examples are the rhodium-catalyzed hydroformylation by dinuclear complexes[2] or the activation of alkynes by gold complexes.[3] In general, gold catalysis,[4] and especially dinuclear gold complexes, have attracted significant attention due to their high catalytic activity.[5–7] Gold complexes have proved particularly suitable as catalysts for the hydroamidation of olefins,[8,9,9b,10] allowing the reaction to proceed even under mild conditions (60–90 °C). Some intermolecular hydroamidations[11] have been reported in which dinuclear gold complexes were used as catalysts.[12] Although dinuclear gold catalysis has great potential, and synergistic interactions between the gold atoms have been identified,[13] such an activation mode has not yet been systematically investigated for hydroamidation reactions.

Here, we present a comparison of readily available mononuclear gold complexes with their dinuclear counterparts in the intermolecular hydroamidation of three selected olefins. The influence of three counterions (OTf^-, $[BF_4]^-$ and $[SbF_6]^-$) on the catalytic efficiency of the mononuclear and the dinuclear catalysts was also investigated.

[a] Karlsruhe Institute of Technology (KIT), Institute for Organic Chemistry,
Fritz-Haber Weg 6, 76131 Karlsruhe, Germany
E-mail: jan.paradies@kit.edu
www.paradies-group.de
[b] Karlsruhe Institute of Technology (KIT), Institute for Inorganic Chemistry,
Engesserstrasse 15, 76131 Karlsruhe, Germany
[c] Technical University of Kaiserslautern, Institute of Physical Chemistry,
Erwin-Schrödinger-Straße, 67663 Kaiserslautern, Germany
[‡] Both author contributed equally.
Supporting information for this article is available on the WWW under http://dx.doi.org/10.1002/ejoc.201402068.

Results and Discussion

As a benchmark reaction, we chose the addition of tosyl amide (**1**) to cyclohexene (**2**) using the conditions reported by He (Figure 1).[11a] We compared the [Ph_3PAuCl] (**3**)/AgOTf catalyst system (Scheme 1) with dinuclear gold complexes derived from common bis(diphenylphosphanyl) ligands.[14] In these experiments, an increased reactivity of [xantphos($AuCl)_2$] (**4**)/AgOTf in comparison to **3**/AgOTf was observed under the reported standard conditions (1:4, **1/2**; 0.5 M, see the Supporting Information, Figure S1). These promising results encouraged us to optimize the reaction conditions. An almost stoichiometric reaction was pursued by using a 1:1.5 ratio (**1/2**) of nucleophile to olefin (Figure 1, a). Under these conditions, the reactions proceeded more slowly with both catalyst systems compared with the reported conditions. However, the xantphos-based dinuclear complex **4** (5 mol-%, corresponding to 10 mol-% Au) provided the product **5** in 80% yield after 25 h, whereas **3** (10 mol-%) gave only 60% yield (Figure 1, a). Further optimization of the reaction conditions using 1,2-dichloroethane (DCE) as solvent and higher concentration (3 M) allowed the catalyst loading to be reduced to 4 mol-% for **3** and 2 mol-% for **4** with even shorter reaction times. Similar yields (64 and 82%) were obtained within only 4 h compared with 25 h (Figure 1, b), confirming the superior performance of the dinuclear gold complex **4** when compared with the mononuclear catalyst **3**.

Control experiments showed that the reaction did not proceed in the absence of gold complexes. Two equivalents of silver salts in combination with **4** were required for high catalytic activity.[15] The catalytic hydroamination of cyclohexene (**2**) with sulfonamide **1** using 2 mol-% **4** and 2 mol-% AgOTf or Ag[SbF_6] (2:1, Au/Ag) did not exceed 11% yield of **5** after 5 h. Although the activity of silver complexes in hydroamination reactions has been reported,[16] the employed silver salts did not catalyze the reaction either

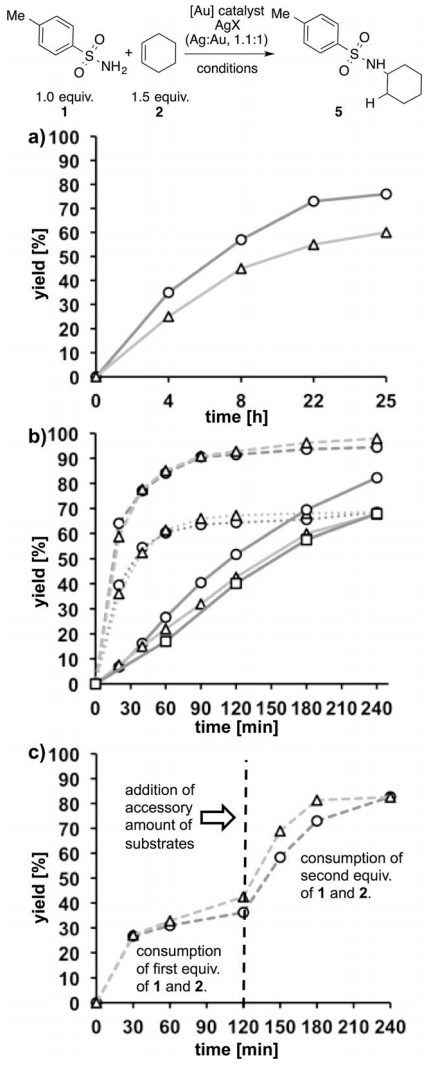

Figure 1. Hydroamidation of cyclohexene (**2**) with tosylamide (**1**); conditions: AgX/Au, (1.1:1), **2** (1.5 equiv.), **1** (1.0 equiv.); X = OTf^- (solid line), $[BF_4]^-$ (dotted line), $[SbF_6]^-$ (dashed line). (a) X = OTf^-; 10 mol-% **3** (triangles), 5 mol-% **4** (circles); 0.5 M; toluene; 85 °C; (b) 4 mol-% **3** (triangles), 2 mol-% **4** (circles), 4 mol-% **6** (squares); 3.0 M; DCE; 85 °C; (c) X = $[SbF_6]^-$; 4 mol-% **3** (triangles); 2 mol-% **4** (circles); 3.0 M; DCE; 85 °C and accessorily added substrates (1.0 equiv. **1**, 1.5 equiv. **2**) after 120 min; yields were determined by GC with dodecane as internal standard.

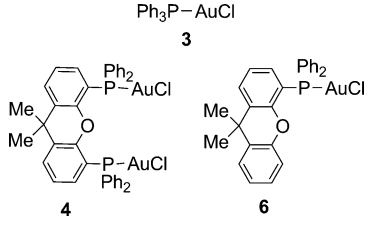

Scheme 1. Mono- and dinuclear gold complexes.

in the absence or presence of xantphos under the optimized reaction conditions. This observation also suggests that HOTf, which is a catalyst for the hydroamidation, is not generated in situ from the silver-mediated decomposition of DCE.[17] Other observations render the Brønsted acid catalyzed hydroamidation[18] unlikely: Firstly, the efficiency of the reaction of cyclohexene (**2**) with tosyl amide (**1**) is phosphine-dependent.[19,20] The impact of the xanthene backbone on the catalytic reaction was probed. Thus, we synthesized xanthene-derived monophosphine[21] gold complex **6** (Scheme 1), which was fully characterized and the solid-state structure was established by single-crystal X-ray diffraction. The molecular structure of **6** (Figure 2) is similar to the molecular structure of $[Ph_3PAuCl]$,[22] exhibiting exclusively κ^1P-coordination. The P1–Au1 distance of 2.224(9) Å is comparable to that of the Ph_3P-system [2.232(4) Å], whereas the Au1–Cl1 distance is reduced by 18 pm to 2.273(1) Å. As anticipated, **6** and **3** exhibit identical catalytic performances when activated with AgOTf (Figure 1, b), which can be attributed to their similar structures. Thus, it is reasonable to suggest that the increased activity observed for **4** is a result of the spatial orientation/proximity of the two gold atoms.

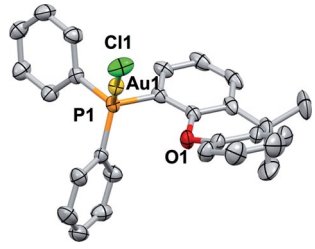

Figure 2. Molecular structure of **6** (hydrogen atoms are omitted for clarity; thermal ellipsoids are drawn at the 50% probability level); selected bond lengths and angles: P1–Au1 2.224(9) Å, Au1–Cl1 2.273(1 Å), P1–Au1–Cl1 178.3(2)°.

Secondly, substrates that form tertiary carbocations upon protonation, e.g., 1-methylcyclohexene or 2-methylundec-1-ene, undergo hydroamidation in low yield (see the Supporting Information Scheme S1a and b).[18b] Furthermore 3-phenyl-1-propene, a substrate that is susceptible to Brønsted-acid catalyzed isomerization, was subjected the gold-catalyzed hydroamidation with tosyl amide, however, the reaction furnished exclusively the direct addition product, and the byproduct arising from the addition of **1** to isomerized starting material was not observed (see the Supporting Information Figure S1, Scheme S1c).

Thirdly, we compared the efficiency of the gold-catalysts with the various Brønsted-acid catalysts, e.g., HOTf, $H[BF_4]$, $H[PF_6]$, $HNTf_2$, and $H[SbF_6]$ in the hydroamidation of **2** with **1** in toluene and 1,2-dichloromethane. The reaction profiles of the Brønsted-acid catalyzed reaction differ substantially from that of the gold-catalyzed reaction (see the Supporting Information Figures S2–S4). Whereas HOTf outperformed the gold-catalysts in toluene for the reaction of **1** with **2**, the reaction was faster with the gold-catalysts in DCE (also in the presence of xantphos). In the case of $H[BF_4]$, both gold catalysts displayed by far superior reactivity in toluene and DCE. $H[PF_6]$ was ineffective as a Brønsted-acid catalyst in the hydroamidation of **1** with **2**. The two gold catalysts were also ineffective, which can be explained by the formation of coordinatively saturated $[(Ph_3P)_2Au]^+$ or $([xantphos)_2Au_2]^+$ species (see below). The

activation of the gold-catalysts by $AgNTf_2$ also furnished catalytically inactive bisligated gold complexes (see below). However, $HNTf_2$ proved to be an efficient Brønsted-acid catalyst for the hydroamidation of cyclohexene (**2**) by tosyl amide (**1**). Consequently, $HNTf_2$ was not generated along the decomposition pathway of $AgNTf_2$-activated gold complexes.

Finally $H[SbF_6]$ was compared with the $Ag[SbF_6]$ activated gold complexes. The Brønsted-acid proved to be an inefficient catalyst for the hydroamidation (16% after 90 min). In contrast, the gold complexes provided the product in 90% yield after 90 min. The collected data supports the conclusion that the hydroamidation of **2** with **1** is catalyzed by cationic gold-species.

One key step of the hydroamidation reaction is the activation of the double bond by cationic gold complexes.[23] Consequently, catalysts containing strongly coordinating anions[24] should display lower rates than catalysts with weaker coordinating anions. Indeed, the activation of the two precatalysts **3** and **4** by AgOTf, $Ag[BF_4]$, and $Ag[SbF_6]$ led to very different kinetic profiles (Figure 1, b). Catalytic reactions employing $[BF_4]^-$ as anion had higher initial rates than those with OTf^-. However, when $[BF_4]^-$ was used, both the mononuclear (**3**) and dinuclear (**4**) catalyst precursors displayed identical productivity (68% after 4 h). The same trend was observed for the $Ag[SbF_6]$-activated catalysts, albeit with dramatically increased reactivity. The intermolecular hydroamidation using **3**/$Ag[SbF_6]$ or **4**/$Ag[SbF_6]$ as catalysts provided the product **5** in essentially quantitative yields [95 and 98% (GC yield); 99 and 99% (isolated yield)] within 4 h. The high catalytic activity of both gold complexes after $Ag[SbF_6]$-activation was maintained during the course of the reaction, as shown by the addition of an extra equivalent of olefin and nucleophile after 120 min (Figure 1, c). The first equivalent of reactants (1.5 mmol **2**, 1.0 mmol **1**) were consumed in the first half of the reaction, giving rise to 72 and 84% yield for the first equivalents (36 and 42% overall yield; referenced to 2 mmol product **5**; Figure 1, c). After 120 min, a second equivalent of reactants was added and the hydroamidation product **5** was produced with the same efficiency (82% for both catalysts). The conversion of sequentially added starting material demonstrates the integrity of the catalytically active species over the reaction time. The small difference in reactivity (12%) of the PPh_3 and xantphos systems revealed in Figure 1 (b) was attributed to changes in concentration upon addition of a supplemental amount of substrate.

The dramatic change of reactivity of both $[SbF_6]$-derived catalysts may be understood in terms of the coordinating ability of the anion. It is well-known that weakly coordinating anions can be categorized by their fluoride ion affinity (FIA).[25] Accordingly, $[SbF_6]^-$ (489 kJ/mol FIA) is a weaker coordinating anion than $[BF_4]^-$ (338 kJ/mol FIA). Thus, the $[SbF_6]^-$ anion is more easily replaced by an olefin than $[BF_4]^-$, providing higher catalytic activity. In this case, the amount of catalytically active metal sites for the employed systems **3**/$Ag[SbF_6]$ and **4**/$Ag[SbF_6]$ is identical (in both cases 4 mol-%), which leads to identical efficiencies (cf. Figure 1, b, dashed line). On the other hand, density functional theory (DFT) calculations predicted tighter binding affinities to the $[Ph_3PAu]^+$ entity for the OTf^- anion than for $[BF_4]^-$.[23] The increased rates of the dinuclear catalyst system **4**, having OTf^- as anion, strongly support an activation step in which the substitution of an anion is facilitated by the presence of the second metal center. Such processes are significantly influenced by the nature and polarity of the solvent, giving rise to tight, loose, or solvent-separated ion pairs with different catalytic reactivity. This may explain the rate increase when the solvent was changed to a more polar one (toluene $\varepsilon = 2.38$; DCE $\varepsilon = 10.42$). Alternatively, the toluene can coordinate to the electrophilic gold center through the aromatic ring, competing with coordination of the olefin.

We then investigated whether the anion-dependent activity of the gold-catalysts were also observable with other substrates. 1-Octene (**7**) was chosen as a challenging substrate for the intermolecular hydroamidation, the transformation of which leads to a mixture of three isomers, which has also been observed in related gold-catalyzed addition reactions.[11a,26] Indeed, when **3** and **4** were employed as catalyst precursors in combination with the corresponding silver salts, different reactivities were observed (Figure 3, a, solid, dotted, and dashed lines). In this case, $[SbF_6]^-$ also proved to be the best counterion for the transformation. The product **8** was obtained in 98 and 85% yield with **3** and **4**, respectively (isolated yield of mixture of isomers after 10.5 h: 99% for **3**, 90% for **4**). Using $[BF_4]^-$ as anion, lower yields (55 and 23%) were obtained, with the Ph_3P-system being the more active catalyst. Interestingly, when **3** or **4** were activated with AgOTf, comparable activities for the two catalysts were observed. As a third olefin, we investigated norbornene (**9**) as substrate for the intermolecular hydroamidation using only a 1.03:1.0 ratio of olefin to nucleophile even at a reduced temperature of 75 °C (Figure 3, b). The two catalyst precursors were employed in the reaction after activation with the corresponding silver salt. In all cases, the dinuclear complex showed the highest initial rates (Figure 3, b). The reactivity increased in the order $[BF_4]^- < OTf^- < [SbF_6]^-$ for both catalysts. The mononuclear Ph_3P-system **3** displayed an induction period with all counterions. Interestingly, the reaction rate increased as soon as approximately 5% of the product was formed, which suggests that the product might be involved in a turnover-limiting step, presumably the proton transfer. The reactivity of the $[SbF_6]^-$ and OTf^- derived catalysts were comparable, whereas the $[BF_4]^-$ system required 240 min for completion. In contrast, the dinuclear catalyst system **4**/$Ag[SbF_6]$ produced the intermolecular hydroamidation product **10** in quantitative yield (83% isolated yield) within only 20 min.

Although the catalytic systems feature divergent reactivity, some mechanistic considerations can be made: (1) the hydroamidation reaction proceeds more efficiently in polar solvents: the stabilization of the cationic or dicationic metal complex is favored in a polar solvent and the replacement by the olefin is facilitated. This is in agreement with the

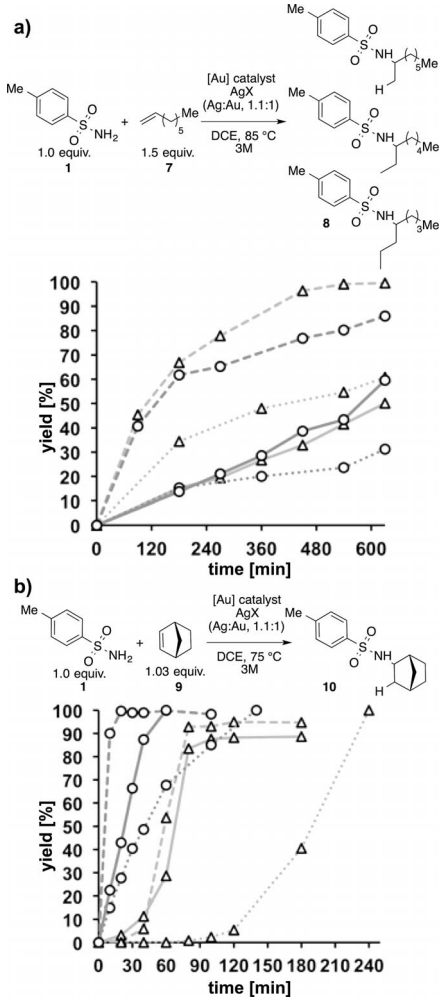

Figure 3. (a) Hydroamidation of 1-octene (**7**) with tosylamide (**1**); conditions: AgX/Au, (1.1:1), **7** (1.5 equiv.), **1** (1.0 equiv.); X = OTf^- (solid line), $[BF_4]^-$ (dotted line), $[SbF_6]^-$ (dashed line); 4.0 mol-% **3** (tringles); 2.0 mol-% **4** (circles); 3.0 M; DCE; 85 °C; (b) hydroamidation of norbornene (**9**) with tosylamide (**1**); conditions: AgX/Au, (1.1:1), **9** (1.03 equiv.), **1** (1.0 equiv.); X = OTf^- (solid line), $[BF_4]^-$ (dotted line), $[SbF_6]^-$ (dashed line); 2 mol-% **3** (triangles), 1.0 mol-% **4** (circles); 3.0 M; DCE; 75 °C; yields were determined by GC analysis with dodecane as internal standard.

observation that (2) more tightly binding anions diminish the reaction rate. The FIA of $[SbF_6]^-$ is higher than that of $[BF_4]^-$; thus the latter can be classified as a more tightly binding anion, making its displacement by the olefin more difficult. Hence, lower reaction rates were observed for both catalysts. The OTf^- anion displays higher coordination ability than the other two counterions, resulting in lower reaction rates for cyclohexene and 1-octene (cf. Figures 1 and 2, a). Because cationic gold species are generated, which are stabilized by the monophosphine PPh_3 and by the rigid bisphosphine xantphos (3) the relative spatial orientation of the metal atoms and the counterions is a determinant of the reactivity.

According to these considerations, the use of even weaker binding anions such as Tf_2N^- or $[Al(OCH(CF_3)_2)_4]^-$ should result in even more active catalysts. However, the reaction of **4** with $AgNTf_2$ or $Ag[Al(OCH(CF_3)_2)_4]$ resulted in decomposition to the previously reported, coordinatively saturated, and thus catalytically inactive, $[xantphos(Au)]_2^{2+}$ dication **11** ($^{31}P\{^1H\}$ NMR: δ = 34 ppm).[27] For comparison, [**11**]$(ClO_4)_2$ was independently accessed by the reaction of $[Au(tht)ClO_4]$ (tht = tetrahydrothiophene) with xantphos in 76% yield and was characterized by crystal X-ray diffraction analysis (Figure 4). The interatomic Au1–Au2 distance is slightly shorter in [**11**]$(ClO_4)_2$ than in the corresponding nitrate structure (2.829(1) vs. 2.858(1) Å).[28] Both gold atoms are in an essentially linear coordination environment, with P–Au–P angles slightly smaller than 180° (163.50° and 164.53°). The P–Au–P angle is distorted from the ideal 180° geometry by 16.50(6)° and 15.5(2)° [ref. P–Au–P 160.8(1)][28] due to the attractive aurophilic Au–Au interaction.

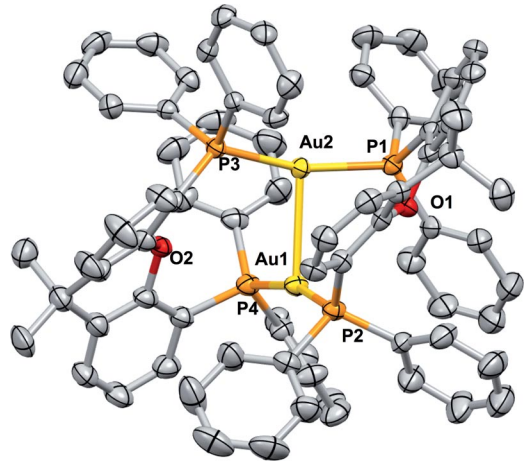

Figure 4. Molecular structure of $[xantphos(Au)]_2(ClO_4)_2$ (hydrogen atoms, disordered counterion and solvent molecules are omitted for clarity; thermal ellipsoids are drawn at the 50% probability level); selected bond lengths and angles: Au1–Au2 2.829(1) Å, Au1–P2 2.328(2) Å, Au1–P4 2.331(2) Å, Au2–P3 2.319(2) Å, Au2–P1 2.333(2) Å, P1–Au2–P3 163.5(2)°, P2–Au1–P4 164.5(6)°.

To shed some light on the nature of the gold species involved in the catalytic process, a series of $^{31}P\{^1H\}$ NMR experiments were performed. The reaction of the mononuclear [xantphos(AuCl)][29] complex **12** with AgOTf furnished [**11**]$(OTf)_2$ exclusively, as evidenced by ^{31}P NMR spectroscopy (Scheme 2). Consequently, cationic **12** can be excluded as a potential catalytically active species. We then turned our attention to the corresponding dinuclear gold complex **4**. The $^{31}P\{^1H\}$ NMR spectrum of the reaction mixture of **4** with two equivalents of AgOTf featured three signals with chemical shifts of δ = 29.6, 20.0, and 17.0 ppm (see the Supporting Information Figure S5). The resonance at δ = 20.0 ppm was assigned to the dicationic gold complex $[xantphos(Au)_2]^{2+}$.[28] However, the complex nature of the mixture prevented the application of pulsed-gradient spin-echo (PGSE) diffusion experiments to establish the dinuclear nature of the catalytically active species. In the absence of olefin and sulfonamide, the species decomposed within a short time at room temperature (Figure S6). This decomposition is accompanied by the formation of a gold mirror

and a decrease of intensity of the signal at δ = 20.0 ppm. Concomitantly, among others, a broader signal appeared at δ = 34 ppm, which corresponds to the catalytically inactive dinuclear complex [xantphos(Au)]$_2X_2$,[27] as confirmed by NMR experiments performed at 233 K. This decomposition pathway is known for the parent $[Ph_3PAu]^+$ system, leading to catalytically inactive $[(Ph_3P)_2Au]^+$. When either olefin or nucleophile is added, a different composition of mixture is observed. Whereas the olefin promotes the formation of multiple species featuring signals at significantly higher frequencies (δ > 40 ppm),[30] the addition of the nucleophile stabilizes the dicationic species and prevents the formation of the catalytically inactive [xantphos(Au)]$_2^{2+}$ dication **11** (Figures S7–S8).

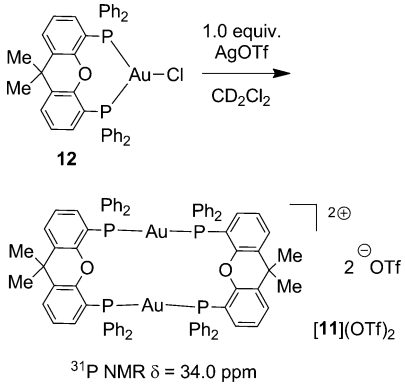

Scheme 2. Formation of [**11**](OTf)$_2$ from **12**.

Finally, ESI-MS experiments were conducted with the aim of characterizing the intermediates of the catalytic hydroamidation of cyclohexene (**2**) with tosylamide (**1**). However, conclusive results could not be obtained from analysis of the reaction mixture. Nevertheless, the dinuclear **4**/Ag[SbF_6] system could be analyzed in the hydroalkoxylation of phenylpropyne (**13**) (Figure 5).[31] The mass spectra (positive ion mode) displayed signals at *m*/*z* 775 for [xantphos(Au)]$^+$ and *m*/*z* 1007 for [xantphos(AuCl)(Au)]$^+$. As evidenced before, [xantphos(Au)]$^+$ is not a competent catalyst for the hydroamination, and readily dimerizes in solution (see Scheme 2). Likewise, [xantphos(AuCl)(Au)]$^+$ can be excluded as an active species because two equivalents of silver salt are required for efficient hydroamidation reaction (see above). Remarkably, a signal at *m*/*z* 1119 was recorded that was assigned to the monocationic dinuclear geminal diaurated complex **14** (Figure 5).[32] Collision-induced dissociation experiments with mass-selected **14** showed the loss of *m*/*z* 344 (assigned to [($C_{10}H_{11}O$)(Au)]) with a remaining complex at *m*/*z* 775 (assigned to [xantphos(Au)]$^+$). An additional fragmentation channel showed the loss of *m*/*z* 359 (assigned to [(($C_{10}H_{11}O$)CH_3)(Au)]), resulting in a mass signal at *m*/*z* 760 (assigned to [(xantphos-CH_3)(Au)]$^+$) (see Figures S9–11, Supporting Information). The observation of intermediate **14** confirms that [xantphos($AuCl)_2$] is converted into the dicationic species upon reaction with 2 equiv. Ag[SbF_6], which is in accordance with the NMR experiments. This bimetallic dicationic species is able to activate multiple bonds, as evidenced by ESI-MS and is tentatively assigned as the active species in the hydroamidation.

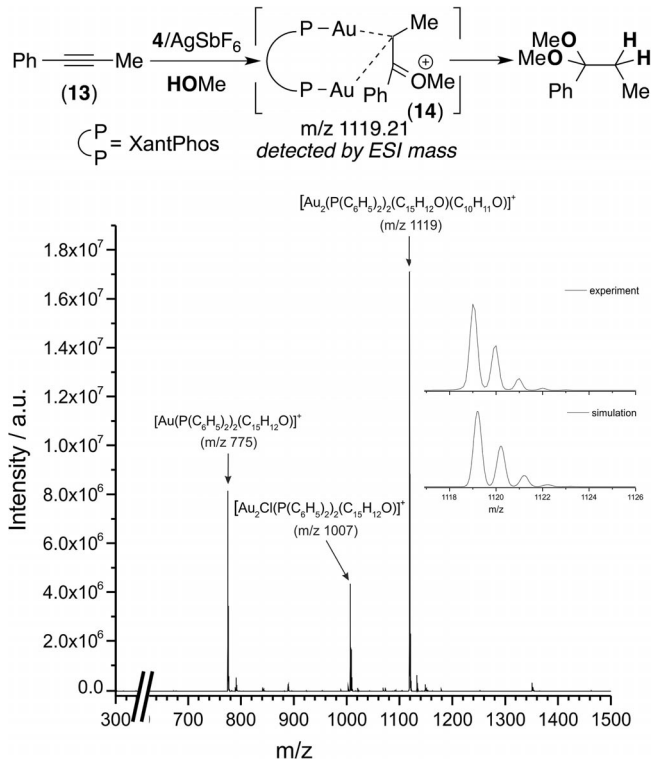

Figure 5. Hydroalkoxylation of phenylpropyne (**13**).

Conclusions

Dinuclear dicationic [xantphos($Au)_2$]$^{2+}$ serves as a starting point for a tentative explanation for the observed reactivity. The increased reactivity of this species for selected substrates might be explained by increased electrostatic interactions with olefins or nucleophiles (evidenced by increased stability of [xantphos($Au)_2$]$^{2+}$ in the presence of **1**). The propensity of the anion to coordinate to the cationic gold centers accounts for counterion effects and can be compensated for by strong olefinic donors, e.g., cyclohexene and norbornene. The location of anions in gold–olefin or gold–alkyne complexes is dependent on both the coordinated ligand and the counterion.[24,33] For dicationic gold–olefin complexes this situation becomes even more pronounced because two counterions must be accommodated in the outer coordination sphere, having a stronger impact on the reaction (as observed for OTf).

The catalytic intermolecular hydroamidation of olefins was developed by taking advantage of mononuclear and dinuclear catalyst systems. Our new system is active with a reduced catalyst loading and at higher concentration. Unprecedented activity was observed for the reaction of norbornene and sulfonamide catalyzed by the xantphos–gold system. However, it was found that such accelerating effect is highly sensitive to several factors, namely the chosen

anion, solvent, and substrate. The characterization of the catalytically active species and its application in other transformations will be the focus of future studies in our laboratories.

Experimental Section

[Ph_3PAuCl] (**3**), [xantphos$(AuCl)_2$] (**4**), and [(4-(diphenylphosphanyl)-9,9-dimethylxanthene)(AuCl)] (**6**) were prepared according to reported procedures[34] by the reaction of one equivalent [(tht)AuCl] (tht = tetrahydrothiophene) per phosphino unit with the corresponding phosphine.

[4-(Diphenylphosphanyl)-9,9-dimethylxanthene]AuCl (6): To a solid mixture of 4-(diphenylphosphanyl)-9,9-dimethylxanthene (1.0 equiv., 60 mg, 0.15 mmol) and (tht)AuCl (1.0 equiv., 48 mg, 0.15 mmol), anhydrous CH_2Cl_2 (7 mL) was added and the mixture was stirred in the dark overnight. The solvent was removed in vacuo and the solid was washed with a mixture of CH_2Cl_2 and Et_2O (1:10, 1.5 mL), to deliver the product as a white solid in quantitative yield (94 mg). ^{1}H NMR (300 MHz, $CDCl_3$): δ = 7.69–7.61 (m, 5 H), 7.56–7.43 (m, 6 H), 7.38–7.33 (m, 1 H), 7.12–7.03 (m, 3 H), 6.8 (ddd, ^1J = 13.1, ^2J = 7.3, ^2J = 1.2 Hz, 1 H), 6.63–6.58 (m, 1 H), 1.61 (s, 6 H) ppm. $^{13}C\{^1H\}$ NMR (75 MHz, $CDCl_3$): δ = 152.29 (d, $J_{C,P}$ = 3.7 Hz), 149.57, 134.29 (d, $J_{C,P}$ = 15.0 Hz),132.43 (d, $J_{C,P}$ = 7.5 Hz), 131.95 (d, $J_{C,P}$ = 2.8 Hz), 130.49 (d, $J_{C,P}$ = 2.2 Hz), 129.76, 129.28 (d, $J_{C,P}$ = 12.3 Hz), 129.15, 128.30, 127.78, 125.52, 124.13, 123.47, 123.32, 116.62, 34.5 (d, $J_{C,P}$ = 1.1 Hz), 31.79 ppm. $^{31}P\{^1H\}$ NMR (101.2 MHz): δ = 26.07 (s) ppm. HRMS (EI): *m/z* calcd. for $C_{27}H_{23}POClAu$ $[M]^+$ 626.0835; found 626.0832. $C_{27}H_{23}AuClOP$ (626.87): calcd. C 51.73, H 3.70; found C 51.48, H 3.71. Suitable crystals for X-ray diffraction analysis were obtained from slow diffusion of pentane into a saturated solution of **6** in CH_2Cl_2. Crystallographic data can be obtained free of charge from the Cambridge Crystallographic database (CCDC-966105).

[Xantphos(Au)]$_2$[ClO$_4$]$_2$ [11](ClO$_4$)$_2$: Xantphos (1.00 equiv., 200 mg, 0.35 mmol) and [Au(tht)$_2$]ClO$_4$ (1.12 equiv., 160 mg, 0.39 mmol) were dissolved in CH_2Cl_2 (10 mL) and the solution was stirred for 2 h in the dark. The solvent was concentrated (ca. 6 mL) under vacuum and pentane (15 mL) was added to precipitate the product, which was isolated as a white crystalline solid (230 mg, 0.13 mmol, 76% yield). ^{1}H NMR (300 MHz, $CDCl_3$): δ = 7.96 (m, 2 H), 7.67 (br. s, 2 H), 7.49 (m, 6 H), 7.25 (br. s, 4 H), 6.97 (m, 10 H), 6.25 (br. s, 2 H), 1.87 (br. s, 6 H) ppm. $^{13}C\{^1H\}$ NMR (75 MHz, $CDCl_3$): δ = 133.45, 133.05, 130.66, 130.32, 129.79, 35.32 ppm. $^{31}P\{^1H\}$ NMR (101.2 MHz): δ = 34.49 (br. s) ppm. HRMS (EI) could not be obtained due to fast decomposition of **11** in the gas phase. Suitable crystals for X-ray diffraction were obtained as colorless needles by slow diffusion of pentane into a solution of [**11**](ClO$_4$)$_2$ in CH_2Cl_2. Crystallographic data can be obtained free of charge from the Cambridge Crystallographic database (CCDC-966106).

Catalytic Hydroamidation of Olefins. Typical Procedure: All experiments were carried out on 1 mmol-scale of tosylamide (**1**). To a solid mixture of the corresponding gold compound [Ph_3PAuCl] (**3**; 19.8 mg, 0.040 mmol, 4.0 mol-%) or [xantphos$(AuCl)_2$] (**4**; 20.9 mg, 0.020 mmol, 2.0 mol-%) and the corresponding silver salt (Au/Ag = 1:1.1) AgOTf (11.3 mg, 44.0 µmol), $AgSbF_6$ (15.1 mg, 44.0 µmol), or $AgBF_4$ (8.6 mg, 44.0 µmol) in a 10 mL vial, anhydrous DCE (330 µL) under argon atmosphere was added and the mixture was stirred for 30 min. The corresponding olefin cyclohexene (123 mg, 152 µL, 1.50 mmol, 1.50 equiv.), norbornene (97.0 mg, 1.03 mmol, 1.03 equiv.), or 1-octene (168 mg, 240 µL, 1.50 mmol, 1.50 equiv.) was added, followed by dodecane (172.0 mg, 230 µL, 1.00 mmol, 1.00 equiv.) as internal standard and the mixture was stirred for another 5–10 min. Finally, **1** (171.2 mg, 1.00 mmol, 1 equiv.) was added, the vial was sealed and immediately taken to 85 °C (75 °C in the case of norbornene) while stirring for the time specified. To follow the formation of hydroamidation products in real time, samples (ca. 40–50 µL) were taken at the specified time intervals and immediately loaded on aluminum oxide columns (ca. 2 cm) packed in Pasteur pipettes. A solution of the reaction mixture was obtained by using EtOAc/Et_2O (10 mL, 1:1 v/v) to carry the mixture throughout the short column and then a sample was injected on the GC. Relative yields of products were determined by comparison between the area corresponding to the products and that of the dodecane.

***N*-Cyclohexyl-4-methylbenzenesulfoneamide (5):** According to the general procedure, the reaction of $TsNH_2$ (**1**; 1.0 mmol) with cyclohexene (**2**; 1.5 mmol) using the [xantphos$(AuCl)_2$]/$AgSbF_6$ catalyst system composed of **4** (20.9 mg, 20.0 µmol, 2.00 mol-%) and $AgSbF_6$ (15.1 mg, 44.0 µmol, 4.40 mol-%), was stopped after 240 min and immediately subjected to column chromatography using aluminum oxide as stationary phase (EtOAc/cyclohexane, 1:9 to 1:4) to give **5** (244 mg, 0.97 mmol, 97%). ^{1}H NMR (300 MHz, $CDCl_3$): δ = 7.77 (d, J = 8.5 Hz, 2 H), 7.29 (d, J = 8.5 Hz, 2 H), 4.70 (d, J = 7.5 Hz,1 H, NH), 3.18–3.04 (m, 1 H, NCH), 2.42 (s, 3 H, CH_3), 1.75–1.71 (m, 2 H), 1.67–1.59 (m, 2 H), 1.52–1.45 (m, 1 H), 1.28–1.02 (m, 5 H) ppm. $^{13}C\{^1H\}$ NMR (75 MHz, $CDCl_3$): δ = 143.21, 138.61, 129.74, 127.05, 52.68, 34.01, 25.26, 24.75, 21.64 ppm. MS (EI, 70 eV): *m/z* (%) = 254.1 (14) $[M + H]^+$, 253.1 (100) $[M]^+$, 210.0 (99), 155.0 (94) $[C_7H_7O_2S]^+$, 98.1 (60) [M–Ts: $C_6H_{12}N]^+$, 91.1 (53) $[C_7H_7]$.

***N*-Tosyl-2-aminooctane, *N*-Tosyl-3-aminooctane, and *N*-Tosyl-4-aminooctane (8):** According to the general procedure, the reaction of $TsNH_2$ (**1**; 1.0 mmol) and 1-octene (**7**; 1.5 mmol) with the [xantphos$(AuCl)_2$]/$AgSbF_6$ catalyst system consisting of (**4**; 20.9 mg, 0.020 mmol, 2.00 mol-%) and $AgSbF_6$ (15.1 mg, 44.0 µmol, 4.40 mol-%) was stopped after 10.5 h and immediately subjected to column chromatography using aluminum oxide as stationary phase (EtOAc/cyclohexane, 1:9 to 1:4) to give **8** (90% yield, 256 mg; 0.90 mmol) as a mixture of isomers. The ratio of isomers was 1.7:1.5:1.0 as judged by the integration relative to the standard using GC analysis. ^{1}H NMR (300 MHz, $CDCl_3$): δ = 7.70 (br. d, J = 8.3 Hz, 2 H), 7.21 (br. d, J = 8.3 Hz, 2 H), 4.73 (app. t, J = 7.7 Hz, 1 H, NH), 3.20 (overlapped sept, J = 6.9 Hz, 1 H), 3.09 (overlapped sext, J = 6.4 Hz, 1 H), 3.06 (overlapped sext, J = 6.6 Hz, 1 H), 2.34 (s, 3 H, CH_3), 1.42–1.05 (m, 10 H), 0.94 (d, J = 6.3 Hz, 3 H, CH_3), 0.76 (overlapped t, J = 7.0 Hz, 3 H, CH_3), 0.73 (overlapped t, J = 6.9 Hz, 3 H, CH_3), 0.69 (overlapped t, J = 7.2 Hz, 3 H, CH_3) ppm. $^{13}C\{^1H\}$ NMR (75 MHz): δ = 143.13, 143.07, 138.66, 138.64, 138.47, 129.64, 129.57, 127.14, 127.11, 55.45, 53.96, 50.07, 37.49, 37.27, 34.71, 34.43, 31.74, 31.61, 28.98, 27.86, 27.42, 25.52, 24.99, 22.60, 22.54, 22.51, 21.79, 21.55, 18.52, 14.12, 14.01, 13.95, 13.91, 9.64 ppm. MS (EI, 70 eV): *m/z* (%) = 283.2 (12) $[M]^+$, 268.2(5) $[M–CH_3]^+$, 254.1 (73) $[M–C_2H_5]^+$, 240.1 (40) $[M – C_3H_7]^+$, 226.1 (45) $[M – C_4H_9]^+$, 212.1 (57) $[M – C_5H_{11}]^+$, 198.0 (100) $[C_9H_{12}NO_2S]^+$, 155.0 (84) $[C_7H_7O_2S]^+$, 91 (52) $[C_7H_7]$.

***N*-(Bicyclo[2.2.1]heptane-2-yl)-4-methylbenzenesulfoneamide (10):** According to the general procedure, the reaction of $TsNH_2$ (**1**; 1.0 mmol) and norbornene (**9**; 1.03 mmol) using the [xantphos$(AuCl)_2$]/$AgSbF_6$ catalyst system composed of **4** (10.4 mg, 10.0 µmol, 1.00 mol-%) and $AgSbF_6$ (7.56 mg, 22.0 µmol, 2.20 mol-%) was stopped after 20 min and immediately subjected to column

chromatography using aluminium oxide as stationary phase (EtOAc/cyclohexane, 1:9 to 1:4) to give **10** (221 mg, 0.83 mmol, 83% yield). ^{1}H NMR (300 MHz, $CDCl_3$): δ = 7.75 (d, J = 8.0 Hz, 2 H), 7.30 (d, J = 8.0 Hz, 2 H), 4.70 (d, J = 7.2 Hz, 1 H, NH), 3.14–3.08 (m, 1 H, NCH), 2.43 (s, 3 H, CH_3), 2.18 (br. s, 1 H), 2.08 (br. s, 1 H), 1.58 (ddd, ^1J = 12.9, ^2J = 8.0, ^3J = 2.5 Hz, 1 H), 1.42–1.25 (m, 3 H), 1.18–0.91 (m, 4 H) ppm. $^{13}C\{^1H\}$ NMR (75 MHz): δ = 143.34, 138.03, 129.79, 127.22, 56.78, 42.60, 40.89, 35.70, 35.30, 28.13, 26.44, 21.67 ppm. MS (EI, 70 eV): *m/z* (%) = 266.1 (15) $[M + H]^+$, 265.1 (69) $[M]^+$, 210.0 (30), 184.0 (72), 155.0 (88) $[C_7H_7O_2S]^+$, 133.0 (26), 110.1 (100) [M–Ts: $C_7H_{12}N]^+$, 91 (87) $[C_7H_7]^+$, 81.0 (70).

Supporting Information (see footnote on the first page of this article): Synthetic procedures, NMR spectroscopic data, kinetic data, ESI-MS data, X-ray crystallographic data.

Acknowledgments

Financial support by the DFG-funded transregional collaborative research center SFB/TRR 88 [Cooperative Effects in Homo- and Heterometallic Complexes (3MET)] and the Helmholz-Research-School (Energy-Related Catalysis; doctoral fellowship to C. K.) is gratefully acknowledged. The Deutsche Forschungsgemeinschaft (DFG) is acknowledged for a Heisenberg fellowship to J. P.

[1] a) I. Bratko, M. Gomez, *Dalton Trans.* **2013**, *42*, 10664–10681; b) E. K. van den Beuken, B. L. Feringa, *Tetrahedron* **1998**, *54*, 12985–13011; c) J. Park, S. Hong, *Chem. Soc. Rev.* **2012**, *41*, 6931–6943; d) M. Shibasaki, N. Yoshikawa, *Chem. Rev.* **2002**, *102*, 2187–2209.

[2] a) M. E. Broussard, B. Juma, S. G. Train, W. J. Peng, S. A. Laneman, G. G. Stanley, *Science* **1993**, *260*, 1784–1788; b) R. C. Matthews, D. K. Howell, W. J. Peng, S. G. Train, W. D. Treleaven, G. G. Stanley, *Angew. Chem. Int. Ed. Engl.* **1996**, *35*, 2253–2256; c) W. J. Peng, S. G. Train, D. K. Howell, F. R. Fronczek, G. G. Stanley, *Chem. Commun.* **1996**, 2607–2608; d) A. Zanardi, J. A. Mata, E. Peris, *J. Am. Chem. Soc.* **2009**, *131*, 14531–14537; e) S. Gonell, M. Poyatos, E. Peris, *Angew. Chem. Int. Ed.* **2013**, *52*, 7009–7013; *Angew. Chem.* **2013**, *125*, 7147–7151 .

[3] a) A. S. K. Hashmi, I. Braun, P. Nosel, J. Schadlich, M. Wieteck, M. Rudolph, F. Rominger, *Angew. Chem. Int. Ed.* **2012**, *51*, 4456–4460; *Angew. Chem.* **2012**, *124*, 4532–4536; b) A. S. K. Hashmi, M. Wieteck, I. Braun, P. Nosel, L. Jongbloed, M. Rudolph, F. Rominger, *Adv. Synth. Catal.* **2012**, *354*, 555–562; c) Y. Oonishi, A. Gomez-Suarez, A. R. Martin, S. P. Nolan, *Angew. Chem. Int. Ed.* **2013**, *52*, 9767–9771; d) A. S. K. Hashmi, I. Braun, M. Rudolph, F. Rominger, *Organometallics* **2012**, *31*, 644–661.

[4] a) A. S. K. Hashmi, *Chem. Rev.* **2007**, *107*, 3180–3211; b) M. Rudolph, A. S. K. Hashmi, *Chem. Soc. Rev.* **2012**, *41*, 2448–2462; c) A. S. K. Hashmi, M. Rudolph, *Chem. Soc. Rev.* **2008**, *37*, 1766–1775; d) A. S. K. Hashmi, M. Wieteck, I. Braun, M. Rudolph, F. Rominger, *Angew. Chem. Int. Ed.* **2012**, *51*, 10633–10637; *Angew. Chem.* **2012**, *124*, 10785–10789; e) A. S. K. Hashmi, T. Lauterbach, P. Nosel, M. H. Vilhelmsen, M. Rudolph, F. Rominger, *Chem. Eur. J.* **2013**, *19*, 1058–1065; f) P. Nosel, T. Lauterbach, M. Rudolph, F. Rominger, A. S. K. Hashmi, *Chem. Eur. J.* **2013**, *19*, 8634–8641.

[5] A. Pradal, P. Y. Toullec, V. Michelet, *Synthesis* **2011**, 1501–1514.

[6] a) M. P. Munoz, J. Adrio, J. C. Carretero, A. M. Echavarren, *Organometallics* **2005**, *24*, 1293–1300; b) M. J. Johansson, D. J. Gorin, S. T. Staben, F. D. Toste, *J. Am. Chem. Soc.* **2005**, *127*, 18002–18003.

[7] a) H. Davies, J. Briones, *J. Am. Chem. Soc.* **2013**, *135*, 13314–13317; b) W. Zi, D. Toste, *J. Am. Chem. Soc.* **2013**, *135*, 12600–12603.

[8] a) R. A. Widenhoefer, X. Q. Han, *Eur. J. Org. Chem.* **2006**, 4555–4563; b) T. E. Muller, K. C. Hultzsch, M. Yus, F. Foubelo, M. Tada, *Chem. Rev.* **2008**, *108*, 3795–3892.

[9] a) X. Q. Han, R. A. Widenhoefer, *Angew. Chem. Int. Ed.* **2006**, *45*, 1747–1749; *Angew. Chem.* **2006**, *118*, 1779–1781; b) Z. B. Zhang, C. Liu, R. E. Kinder, X. Q. Han, H. Qian, R. A. Widenhoefer, *J. Am. Chem. Soc.* **2006**, *128*, 9066–9073; c) J. L. Mcbee, A. T. Bell, T. D. Tilley, *J. Am. Chem. Soc.* **2008**, *130*, 16562–16571.

[10] a) A. K. Mourad, J. Leutzow, C. Czekelius, *Angew. Chem. Int. Ed.* **2012**, *51*, 11149–11152; *Angew. Chem.* **2012**, *124*, 11311–11314; b) M. C. M. Higginbotham, M. W. P. Bebbington, *Chem. Commun.* **2012**, *48*, 7565–7567; c) C. F. Bender, R. A. Widenhoefer, *Org. Lett.* **2006**, *8*, 5303–5305; d) C. F. Bender, R. A. Widenhoefer, *Chem. Commun.* **2006**, 4143–4144; e) R. E. Kinder, Z. Zhang, R. A. Widenhoefer, *Org. Lett.* **2008**, *10*, 3157–3159; f) Z. Zhang, C. F. Bender, R. A. Widenhoefer, *J. Am. Chem. Soc.* **2007**, *129*, 14148–14149; g) Z. Zhang, C. F. Bender, R. A. Widenhoefer, *Org. Lett.* **2007**, *9*, 2887–2889; h) Z. Zhang, S. D. Lee, R. A. Widenhoefer, *J. Am. Chem. Soc.* **2009**, *131*, 5372–5373; i) P. de Fremont, E. D. Stevens, M. R. Fructos, D.-R. M. Mar, P. J. Perez, S. P. Nolan, *Chem. Commun.* **2006**, 2045–2047; j) S. Gaillard, J. Bosson, R. S. Ramon, P. Nun, A. M. Z. Slawin, S. P. Nolan, *Chem. Eur. J.* **2010**, *16*, 13729–13740.

[11] a) J. L. Zhang, C. G. Yang, C. He, *J. Am. Chem. Soc.* **2006**, *128*, 1798–1799; b) V. Lavallo, G. D. Frey, B. Donnadieu, M. Soleilhavoup, G. Bertrand, *Angew. Chem. Int. Ed.* **2008**, *47*, 5224–5228.

[12] a) M. Kojima, K. Mikami, *Synlett* **2012**, 57–61; b) R. L. LaLonde, B. D. Sherry, E. J. Kang, F. D. Toste, *J. Am. Chem. Soc.* **2007**, *129*, 2452–2453; c) O. Kanno, W. Kuriyama, Z. J. Wang, F. D. Toste, *Angew. Chem. Int. Ed.* **2011**, *50*, 9919–9922; *Angew. Chem.* **2011**, *123*, 10093–10096; d) L. I. Rodriguez, T. Roth, J. L. Fillol, H. Wadepohl, L. H. Gade, *Chem. Eur. J.* **2012**, *18*, 3721–3728; e) M. Rodriguez-Zubiri, C. Baudequin, A. Bethegnies, J.-J. Brunet, *ChemPlusChem* **2012**, *77*, 445–454; f) C. Sarcher, A. Luhl, F. C. Falk, S. Lebedkin, M. Kuhn, C. Wang, J. Paradies, M. M. Kappes, W. Klopper, P. W. Roesky, *Eur. J. Inorg. Chem.* **2012**, 5033–5042.

[13] E. Tkatchouk, N. P. Mankad, D. Benitez, W. A. Goddard, F. D. Toste, *J. Am. Chem. Soc.* **2011**, *133*, 14293–14300.

[14] V. Pawlowski, H. Kunkely, A. Vogler, *Inorg. Chim. Acta* **2004**, *357*, 1309–1312.

[15] The hydroamination reaction of **1** with **2** in the presence of **4** activated with $Ag[SbF_6]$ (1 equiv.) only led to yields below 10% of **5**; ligand and silver effects have been identified in gold-catalyzed transformations. For Ag effects, see: a) D. Wang, R. Cai, S. Sharma, J. Jirak, S. K. Thummanapelli, N. G. Akhmedov, H. Zhang, X. Liu, J. L. Petersen, X. Shi, *J. Am. Chem. Soc.* **2012**, *134*, 9012. For ligand effects, see: b) W. Wang, G. B. Hammond, B. Xu, *J. Am. Chem. Soc.* **2012**, *134*, 5697; for a review, see: D. J. Gorin, B. D. Sherry, F. D. Toste, *Chem. Rev.* **2008**, *108*, 3351.

[16] a) J. W. Sun, S. A. Kozmin, *Angew. Chem. Int. Ed.* **2006**, *45*, 4991–4993; *Angew. Chem.* **2006**, *118*, 5113–5115; b) D. J. Ye, X. Zhang, Y. Zhou, D. Y. Zhang, L. Zhang, H. S. Wang, H. L. Jiang, H. Liu, *Adv. Synth. Catal.* **2009**, *351*, 2770–2778; c) V. R. Bhonde, R. E. Looper, *J. Am. Chem. Soc.* **2011**, *133*, 20172–20174; d) V. H. L. Wong, T. S. A. Hor, K. K. Hii, *Chem. Commun.* **2013**, *49*, 9272–9274; e) D. Susanti, F. Koh, J. A. Kusuma, P. Kothandaraman, P. W. H. Chan, *J. Org. Chem.* **2012**, *77*, 7166–7175; f) X. Giner, C. Najera, *Synlett* **2009**, 3211–3213; g) X. Giner, C. Najera, G. Kovacs, A. Lledos, G. Ujaque, *Adv. Synth. Catal.* **2011**, *353*, 3451–3466; h) C. Michon, F. Medina, F. Capet, P. Roussel, F. Agbossou-Niedercorn, *Adv. Synth. Catal.* **2010**, *352*, 3293–3305.

[17] T. T. Dang, F. Boeck, L. Hintermann, *J. Org. Chem.* **2011**, *76*, 9353–9361.
[18] a) Z. G. Li, J. L. Zhang, C. Brouwer, C. G. Yang, N. W. Reich, C. He, *Org. Lett.* **2006**, *8*, 4175–4178; b) D. C. Rosenfeld, S. Shekhar, A. Takemiya, M. Utsunomiya, J. F. Hartwig, *Org. Lett.* **2006**, *8*, 4179–4182.
[19] Asymmetric hydroamidations using chiral phosphine-stabilized gold complexes have also been reported, see ref.[10g,10h,12b]
[20] a) J. Hannedouche, E. Schulz, *Chem. Eur. J.* **2013**, *19*, 4972–4985; b) R. E. M. Brooner, R. A. Widenhoefer, *Chem. Eur. J.* **2011**, *17*, 6170–6178; c) G. Kovacs, A. Lledos, G. Ujaque, *Organometallics* **2010**, *29*, 5919–5926.
[21] M. J. L. Tschan, H. Launay, H. Hagen, J. Benet-Buchholz, P. W. N. M. van Leeuwen, *Angew. Chem.* **2004**, *116*, 2116–2142; M. J. L. Tschan, H. Launay, H. Hagen, J. Benet-Buchholz, P. W. N. M. van Leeuwen, *Chem. Eur. J.* **2011**, *17*, 8922–8928.
[22] A. O. Borissova, A. A. Korlyukov, M. Y. Antipin, K. A. Lyssenko, *J. Phys. Chem. A* **2008**, *112*, 11519–11522.
[23] G. Kovacs, G. Ujaque, A. Lledos, *J. Am. Chem. Soc.* **2008**, *130*, 853–864.
[24] D. Zuccaccia, L. Belpassi, A. Macchioni, F. Tarantelli, *Eur. J. Inorg. Chem.* **2013**, 4121–4135.
[25] I. Krossing, I. Raabe, *Angew. Chem. Int. Ed.* **2004**, *43*, 2066–2090.
[26] X. Zhang, A. Corma, *Chem. Commun.* **2007**, 3080–3082.
[27] G. Tarkanyi, P. Kiraly, G. Palinkas, A. Deak, *Magn. Res. Chem.* **2007**, *45*, 917–924.
[28] A. Deak, T. Megyes, G. Tarkanyi, P. Kiraly, L. Biczok, G. Palinkas, P. J. Stang, *J. Am. Chem. Soc.* **2006**, *128*, 12668–12670.
[29] H. Ito, T. Saito, T. Miyahara, C. M. Zhong, M. Sawamura, *Organometallics* **2009**, *28*, 4829–4840.
[30] R. E. M. Brooner, T. J. Brown, R. A. Widenhoefer, *Chem. Eur. J.* **2013**, *19*, 8276–8284.
[31] J. Roithová, Š. Janková, L. Jašíková, J. Váňa, S. Hybelbauerová, *Angew. Chem. Int. Ed.* **2012**, *51*, 8378–8382.
[32] A. Zhdanko, M. E. Maier, *Chem. Eur. J.* **2014**, *20*, 1918–1930.
[33] a) G. Ciancaleoni, L. Biasiolo, G. Bistoni, A. Macchioni, F. Tarantelli, D. Zuccaccia, L. Belpassi, *Organometallics* **2013**, *32*, 4444–4447; b) D. Zuccaccia, L. Belpassi, F. Tarantelli, A. Macchioni, *J. Am. Chem. Soc.* **2009**, *131*, 3170–3171.
[34] R. Uson, A. Laguna, M. Laguna, D. A. Briggs, H. H. Murray, J. P. Fackler, *(Tetrahydrothiophene)gold(I) or Gold(III) Complexes in Inorganic Syntheses*, John Wiley & Sons, New York, **2007**, p. 85–91.

Received: February 13, 2014
Published Online: ■

EurJOC European Journal of Organic Chemistry

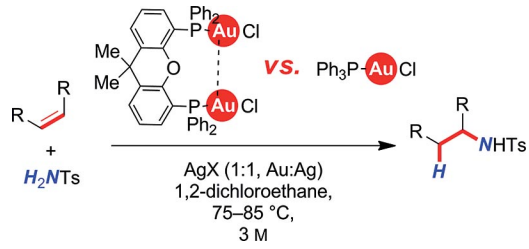

Dinuclear xantphos-derived gold complexes were compared to the mononuclear Ph_3P-gold complex in the hydroamidation of olefins. For some examples, higher activity of the dinuclear gold complexes was observed, suggesting cooperative activation of the substrates.

Keywords: Homogeneous catalysis / Gold / Hydroamination / Dinuclear complexes / Cooperative effects

